AGU PUBLICATIONS

Geophysical Research Letters

RESEARCH LETTER
10.1002/2016GL068233

Key Points:
- Newly observed thrust faulting shows the South Westland Fault Zone (SFWZ) is an active seismogenic structure
- Large but infrequent earthquakes (at least M_w 6.8) with the most recent rupture post −12.1 ± 1.7 ka based on OSL dating
- Intra-Australian Plate faulting shows that key structures remain uncharacterized in areas with rainforest cover

Supporting Information:
- Supporting Information S1
- Movie S1

Correspondence to:
G. P. De Pascale,
snowyknight@gmail.com

Citation:
De Pascale, G. P., N. Chandler-Yates, F. Dela Pena, P. Wilson, E. May, A. Twiss, and C. Cheng (2016), Active tectonics west of New Zealand's Alpine Fault: South Westland Fault Zone activity shows Australian Plate instability, *Geophys. Res. Lett.*, *43*, 3120–3125, doi:10.1002/2016GL068233.

Received 15 FEB 2016
Accepted 12 MAR 2016
Accepted article online 18 MAR 2016
Published online 2 APR 2016

Active tectonics west of New Zealand's Alpine Fault: South Westland Fault Zone activity shows Australian Plate instability

Gregory P. De Pascale[1], Nicholas Chandler-Yates[2], Federico Dela Pena[2], Pam Wilson[2], Elijah May[3], Amber Twiss[3], and Che Cheng[3]

[1]Departmento de Geologia y Centro de Excelencia en Geotermia de Los Andes, Facultad de Ciencias Fisicas y Matematicas, Universidad de Chile, Santiago, Chile, [2]Department of Geological Sciences, University of Canterbury, Christchurch, New Zealand, [3]Fugro Geotechnical (NZ), Christchurch, New Zealand

Abstract The 300 km long South Westland Fault Zone (SWFZ) is within the footwall of the Central Alpine Fault (<20 km away) and has 3500 m of dip-slip displacement, but it has been unknown if the fault is active. Here the first evidence for SWFZ thrust faulting in the "stable" Australian Plate is shown with cumulative dip-slip displacements up to 5.9 m (with 3 m throw) on Pleistocene and Holocene sediments and gentle hanging wall anticlinal folding. Cone penetration test (CPT) stratigraphy shows repeated sequences within the fault scarp (consistent with thrusting). Optically stimulated luminescence (OSL) dating constrains the most recent rupture post-12.1 ± 1.7 ka with evidence for three to four events during earthquakes of at least M_w 6.8. This study shows significant deformation is accommodated on poorly characterized Australian Plate structures northwest of the Alpine Fault and demonstrates that major active and seismogenic structures remain uncharacterized in densely forested regions on Earth.

1. Introduction

Understanding how deformation is partitioned along plate boundary structures is critical for the characterization of seismic hazards and delineation of fault rupture hazard zones. Importantly, the rupture of unknown faults (or those poorly characterized) shows us that building on these structures (i.e., fault rupture hazard) and the shaking generated when they rupture have important financial implications (i.e., cost) in addition to social costs (e.g., the 2010 to the present Canterbury earthquake sequence in New Zealand (NZ)). Much research on plate boundary deformation is focused on the main interplate interface itself (e.g., the Alpine Fault in NZ or the San Andreas Fault in California), with deformation on adjacent intraplate structures being less well characterized, in particular in nonarid areas where dense forests obscure evidence of fault location and activity. The dextral-reverse Alpine Fault forms the boundary between the Australian and Pacific plates in NZ (Figure 1) and is the focus of most regional seismic hazard studies as it is believed to accommodate 50%–80% of the 37 ± 2 mm/yr convergent motion across the plate boundary [*DeMets et al*., 1994; *Sutherland et al*., 2007]. This fault system is seismogenic [*Wells et al*., 1999], although no large earthquakes are documented (since 1840 Common Era) and appears to have both partial ruptures and full ruptures (i.e., not characteristic behavior) [*De Pascale et al*., 2014] resulting in large to great earthquakes (~M_w 7.9–8.3) every 200 to 400 years [e.g., *Sutherland et al*., 2007; *De Pascale and Langridge*, 2012; *Howarth et al*., 2012] and partial ruptures (<M_w 7.9) occurring at unknown intervals between full ruptures. Importantly, because up to 50% of the plate boundary deformation is accommodated on other structures [*Beavan et al*., 1999], these structures contribute to the seismic hazard and should be targeted for characterization to better understand of strain partitioning and seismic hazard. Within the Pacific Plate east of the Alpine Fault, *Cox et al*. [2012] recently identified 110 potentially active faults within the Southern Alps with potential to produce M_w 5.5 to 7.4 earthquakes at recurrence intervals of 1000 to 10,000 years. However the adjacent Australian Plate to the west of the fault is generally considered "stable" in geodetic deformation models [*Wallace et al*., 2007], partially because of the absence of GPS data, with poorly mapped faults with loosely constrained slip rates (due to dense forest and mountainous terrain), as characterized in the National Seismic Hazard Model for NZ [*Stirling et al*., 2012]. The focus of our study is to better understand faults in the Australian Plate adjacent to the Alpine Fault, to improve seismic source models and seismic hazard assessment and to draw attention to other heavily forested regions on Earth where fault activity is perhaps underestimated.

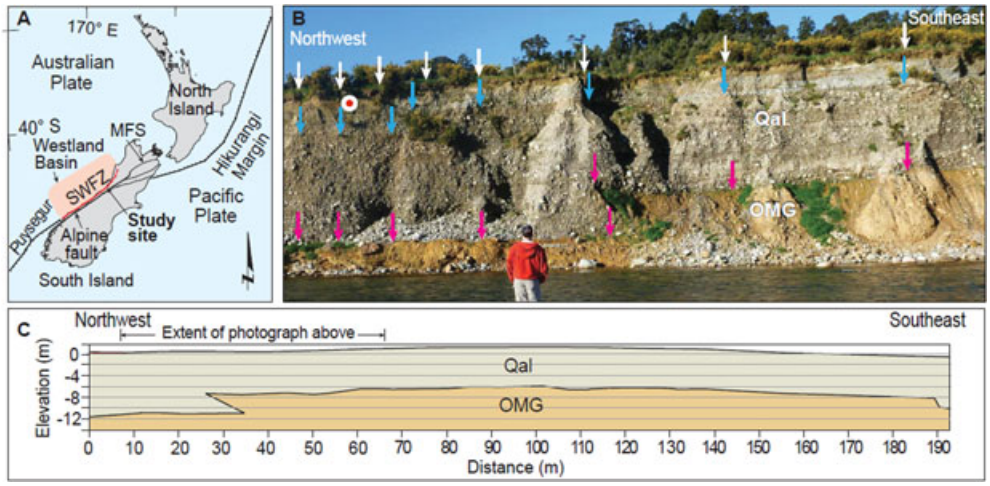

Figure 1. (a) Map of South Island of New Zealand with major structures (i.e., tectonic setting) shown including Westland Basin (red), study site, and Alpine Fault, South Westland Fault Zone (SWFZ as a red fault), Marlborough Fault System (MFS), Hikurangi, and Puysegur margins. (b) Field photograph (looking north) showing the natural exposure along the Mikonui River with the SWFZ-faulted Old Man Gravels (OMG) glacial till (up to the right) with person for scale (~30 m in front). Qal is Quaternary alluvium. Pink arrows indicate the top of the OMG, blue arrows are the top of a clear oxidized layer within the Qal, and white arrows indicate the ground surface all with reverse-sense displacements (red and white circles show OSL sample location). (c) Survey level data showing two main features along the SWFZ: (i) the ground surface (i.e., top of terrace) and (ii) top of OMG till; note the gentle anticlinal folding along both.

2. The South Westland Fault Zone

The South Westland Fault Zone (SWFZ) lies within the 8 to 20 km wide coastal strip and offshore within the Australian plate (i.e., Westland) northwest and subparallel to the Alpine Fault in NZ (Figure 1), although the location is inferred because of a lack of known field exposures and paleoseismic studies [e.g., *Cox and Barrell*, 2007]. The SWFZ is a basin-bounding structure along an elongated sedimentary basin (i.e., the Westland Basin) (Figure 1). The estimated maximum depth of the basin immediately offshore is 3.5 to 4.0 km [*Nathan et al*., 1986]. The cause of Westland Basin subsidence is controversial; *Kamp et al*. [1992] suggest that the basin formed due to flexural downwarping by thrusting along the margin (i.e., a foreland basin with syndepositional thrusting). *Sutherland* [1996] that if a foreland model is applicable to the Westland Basin, then loading of the Australian Plate due to increased Pliocene-Quaternary sediment must have been at least partially due to reverse motion along the SWFZ (i.e., flexural downwarping and thrusting). However, *Walcott* [1998] proposed that the contribution of basin subsidence by thrusting is likely to be small or nonexistent and instead due to isostatic loading that amplifies a preexisting depression without thrusting. Based on apatite age dating [*Kamp et al*., 1992] the uplift rate during the past 1 to 2 Ma was in the range of 4.2–1.4 mm/yr, and based on rapid acceleration in the Quaternary uplift rate (versus 1.0 to 1.2 mm/yr since 10 Ma) while analysis of industry exploration wells [*Sutherland*, 1996] suggests that SWFZ movement started in the middle Miocene. An onshore seismic reflection profile shows basement depth increasing by 2 km adjacent to and 6 km northwest of the Alpine Fault at the SWFZ with which *Davey* [2010] was able to correlate Miocene and younger units within the Westland Basin based on borehole control. Offshore of the SWFZ (adjacent to the Central Alpine Fault), there does not appear to be active faulting based on marine geophysical data [*Barnes and Ghisetti*, 2013]. Gravity data [*Davy et al*., 2013] aid inference of the SWFZ location, where gravity lows are the combined result of SFWZ uplift and large erosional basins and valleys from glaciations. Importantly, the Last Glacial Maximum in NZ occurred between 28 and 20 ka [e.g., *Suggate and Almond*, 2005] when glaciers completely covered most of the SWFZ (i.e., obscuring fault deformation due to erosion and deposition) and in several cases extending beyond the current coastline [*Barrell*, 2011].

3. Methods

We discovered a natural exposure of the SWFZ coincident with the *Davy et al*. [2013] gravity location of the SWFZ along the northern side of the Mikonui River (latitude: −42.909192°; longitude: 170.772736°; adjacent

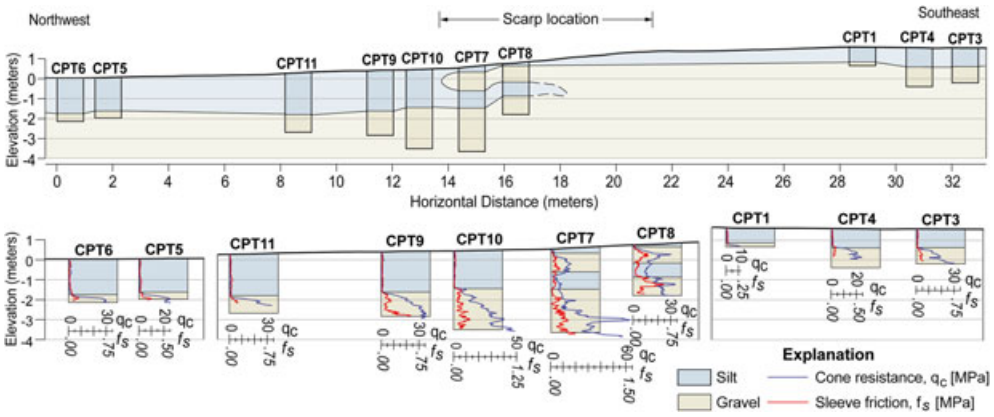

Figure 2. (top) CPT soundings across the GPS-derived topographic profile of the SWFZ scarp as a correlated cross section. Note the repeating sequences within the fault scarp at CPT7 and CPT8 (consistent with thrust faulting), and gravel unit is the same alluvium (Qal) in Figure 1. (bottom) The raw CPT data with cone resistance (q_C; blue line) and sleeve friction (f_S; red line) versus depth with data recorded every 2 cm.

to the SH 6 bridge; Figure 1). The exposure is oriented northwest-southeast with the fault zone located in the middle of this ~400 m long exposure. Here a multidisciplinary approach was successfully used to characterize activity of a thrust fault associated with the SWFZ. Interpretation of available remote imagery combined with field investigations (see supporting information) of a ~ 1 m high scarp that cuts across a fill terrace (and is visible for 140 m across an open paddock before heading into the forest to the northeast) is combined with a natural exposure of subvertical terrace riser formed by erosion along the Mikonui River. Aspects of geometry and displacements of the fault were undertaken both by field measurements and by structure from motion (SfM) techniques of photographic mapping of the exposure using the Autodesk 123D Catch freeware (http://www.123dapp.com/catch). The scarp was profiled to estimate vertical relief using a high-resolution global positioning system (GPS), while a total station was used to determine elevation variability of specific stratigraphic units such as the upper contact of a glacial till unit (Old Man Gravels/Group, OMG, first mentioned by *Gage* [1945]). An optically stimulated luminescence (OSL) sample was collected from the uppermost and faulted unit (Figure 1, in silt at the top of the terrace) to provide insight to event timing. The luminescence was measured during infrared stimulation of fine grain feldspar and used for a multiple aliquot additive dose method (i.e., MAAD, full OSL methodology in the supporting information, and *Chandler-Yates* [2016]).

A subsurface investigation was undertaken using cone penetration testing (CPT). CPTs involve pushing a calibrated cone sensor vertically into the ground at a controlled rate and with continuous electronic measurements to develop a continuous profile. While the cone is being pushed, it measures force on the cone tip (tip resistance, q_C), friction along the sensor sidewalls (sleeve friction, f_s), and the pore water pressure induced in the soil. These measurements are electronically processed, and the separate measurements and ratios are compared to derive a stratigraphic profile, classify soil types, and their distribution [e.g., *Robertson*, 1990], and quantify soil strength. CPTs are increasingly being used to investigate active faults [e.g., *Grant et al.*, 1997; *Marliyani et al.*, 2013] and are especially useful when paleoseismic trenches are not practical. We undertook 10 individual CPT soundings at locations spaced along a transect striking perpendicular to the scarp on the terrace surface 6–10 m back from the top of the river exposure using a 1.2 ton CPT rig with a 15 cm^2 cone (Figure 2: see supporting information). These soundings were compiled and interpreted to develop a correlated geologic fault cross section (Figure 2).

4. Results

The 14 m high terrace riser exposure along the northern bank of the Mikonui River in Westland (Figure 1) contains eolian or overbank silt (silt with sand) overlying an older, yet relatively unweathered (although with conspicuous oxidized layers) cobble-dominated late Otiran (late last glacial, i.e., ~ 18 to 22 ka [e.g., *Almond et al.*, 2001] outwash alluvial sequence (grey to greyish brown, cobble-dominated gravel with light-colored clasts composed of metaargillite, gneiss, and greywacke), undated but estimated based on regional geomorphic mapping and stratigraphy as 14.5 to 40 ka [*Barrell*, 2011]. This outwash itself unconformably overlies

Table 1. SWFZ OSL Age Estimates and Dating Parameters

Sample ID	K (%)	Th (ppm)	U 234Th (ppm)	U 201Pb (ppm)	Water Content (%)	*A* Value	Dose Rate (Gy/ka)	De (Gy)	OSL Age (ka B.P.)
WLL1171	0.86 ± 0.02	6.16 ± 0.09	1.57 ± 0.18	1.21 ± 0.13	19.2	0.073 ± 0.013	0.1945 ± 0.0097	23.77 ± 2.98	12.1 ± 1.7

the Quaternary glacial till and alluvial OMG, moderately weathered clay-rich with a yellowish brown color, clast-supported with schist and greywacke clasts), again undated but estimated as 45 to 360 ka [*Barrell*, 2011]. In this exposure, a thrust fault of the SWFZ strikes northeast (N41E ± 5°) and dips southeast (28° SE) and is relatively well constrained with a clear singular or master fault within a narrow zone defined by fault imbricated cobbles (long axis showing dip slip) within the alluvium between the clear displacements along marker beds. In the lower part of the exposure, the fault offsets clay-rich glacial till in the hanging wall (i.e., OMG, a regionally significant alluvial gold-bearing unit) thrust over younger unconsolidated, well-rounded cobble-dominated alluvium (Figure 1 and supporting information for additional data and field photographs). At the top of the exposure, the cobble-dominated Late Otiran alluvium near the surface is thrust over the silt overbank deposits and this contact is coincident with a scarp on the terrace (see photos in supporting information). Measurements in the field and SfM data show that displacements along the fault trace decrease upward, from the bottom of the exposure, with up to the southeast dip slip of 5.9 m ± 0.1 m (3.0 m ± 0.1 m throw) on the top of the OMG overthrusting the alluvium, 3.7 m ± 0.1 m (1.8 m ± 0.1 m throw) on an oxide horizon in alluvium, and 1.2 m ± 0.1 m (0.5 m ± 0.1 m throw) alluvium thrust over the youngest silt overbank (or loess) deposit. The alluvium overthrusting silt near the top of the exposure is coincident with the up to the southeast ~ 0.7 m to 1.1 m high scarp (possibly degraded from farming) along the terrace at the top of the exposure. OSL dating (Table 1) of the near-surface silt provides an age of 12.1 ± 1.7 ka while our survey of the unit contacts shows gentle anticlinal, hanging wall folding within 170 m of the scarp (Figure 1).

The CPT data (Figure 2) reveal an oftentimes simple two-layer stratigraphy with a 75–90 cm thick, very low tip resistance (<5 MPa) silt unit overlying a gravel/cobble unit (i.e., the alluvium in the exposure) with higher tip resistance values (>5 MPa and up to 50 MPa) to the maximum depth of exploration. Within the scarp, however, the stratigraphy is more complex with repeating overthrust sequences of silt and gravel/cobbles with some with low tip resistance (<5 MPa) layers interspersed between ~ 1 m thick layers of higher tip resistances (from >15 MPa up to 30 MPa) and a very dense basal layer with higher resistances (up to 60 MPa) found up to 4.5 m below ground level (due to cone refusal criteria).

5. Discussion and Conclusions

Our multimethod study of the newly discovered Mikonui River SWFZ exposure, and up to 1.2 m high up to the southeast reverse fault scarp (Figure 1), with CPT subsurface profiling (Figure 2) provides the first evidence of Quaternary activity at one point along the 300 km long SWFZ. The characteristics of the fault and displacements suggest multiple events (at least four) and the most recent rupture here was post 12.1 ± 1.7 ka (Table 1) evidenced by the clear scarp on the terrace. This clear evidence for fault activity demonstrates Quaternary reverse motion along the SWFZ and that plate boundary deformation occurs over a wider zone than previously inferred with modern Alpine Fault footwall (i.e., Australian Plate) uplift along west vergent reverse faults. Because there is no evidence for active faulting west of our site in marine geophysical records [*Barnes and Ghisetti*, 2013], active Australian Plate deformation here is focused in an ~ 20 km zone between the near-shore zone (<1.5 km northwest of the site described here, although no evidence was found for this) and the Alpine Fault (around 18 km away to the southeast at the surface). Importantly, other active faults, including strands of the SWFZ, may exist between our site and the Alpine Fault. Thus, contrary to *Walcott* [1998], the SWFZ is an active structure with stick-slip behavior (i.e., seismogenic and at least M_w 6.8 based on displacement versus magnitude relationships (after *Wells and Coppersmith* [1994]) that aids the formation of the Westland Basin via reverse faulting at the southeast margin as proposed by *Kamp et al.* [1992]. Additionally, the amount of strain partitioned to faults within the SWFZ is significant, which may explain why rates of Australian Plate uplift and the current deformation models do not correlate well. Importantly, if the SWFZ has some amount of strike-slip or oblique motion (i.e., not pure dip slip), the seismogenic potential of the SWFZ is higher than our estimate. Finally, activity of the southern end of the SWFZ is difficult to ascertain from our single site; however, based on the repeated ruptures we document here and the similar stress state

to the south, it is likely that the SWFZ is active there as well. Because some of the SWFZ is located offshore, it is potentially a source of tsunami.

Regionally, *Barth et al*. [2013] used paleontology and stratigraphic age constraints to estimate a geologic Australian plate uplift rate (i.e., the hanging wall of the SWFZ) of ~2.6 mm/yr ~300 km southwest of the Mikonui River, while GPS-derived geodetic data from near our site [*Beavan et al*., 2010] show interseismic SWFZ hanging wall (or other intra-Australian Plate faults) uplift rates of 0.1 mm/yr ± 0.2 mm/yr. This discrepancy suggests coseismic uplift along the SWFZ, and other Australian Plate structures are responsible for uplift of at least 2.3 mm/yr.

In Westland, regional evidence of shaking provides insight into paleo–strong ground motions at a point, including the sedimentary and throw record of *Berryman et al*. [2012] from the Southern Alpine Fault which has a recurrence interval of 329 ± 68 years, whereas the adjacent (<30 km) offshore record shows a recurrence interval for turbidites (i.e., shaking) of ~190 years [*Barnes et al*., 2013]. Importantly, geodetic models (which do not include the SWFZ) [*Wallace et al*., 2007] provide higher Alpine Fault dextral slip rate estimates (30–32 mm/yr) than the dextral geologic slip rates (27 ± 5 mm/yr) [*Norris and Cooper*, 2001], suggesting that other faults may be important here. Newly discovered and likely active faults in the Alpine Fault's hanging wall [*Cox et al*., 2012] and footwall [*Ghisetti et al*., 2014; *Lund Snee et al*., 2013; this study] demonstrate that there are faults capable of generating paleoseismic records which may suggest that Alpine Fault rupture recurrence and slip rates may be lower, highlighting the value of on-fault data for seismic hazard characterization [e.g., *De Pascale et al*., 2014].

The newly discovered SWFZ exposure, scarp, and CPT results show that the Australian Plate, i.e., the footwall of the plate boundary Alpine Fault, is not as stable as previously hypothesized and future research should target these poorly exposed and long faults as these faults represent earthquake sources that need to be factored into seismic source (and rupture hazard) models. Modern remote sensing tools such as lidar and airborne structure from motion (SfM) are extremely helpful for the identification of faults, but oftentimes in densely forested areas, these data are not available or do not work well and thus direct field observations (i.e., field mapping—how we discovered our natural exposure here) provide the best evidence of the location, kinematics, and fault activity for seismic hazard assessments. Ultimately, other regions on Earth with high rates of tectonic deformation and precipitation (with correspondingly dense forest cover, e.g., Papua New Guinea, Indonesia, the Pacific Northwest of North America, and Patagonia) likely have underappreciated as well as unknown and perhaps significant fault zones that require further attention to better understand and mitigate global seismic hazard.

Acknowledgments

Thanks to Brain Anderson for land access, the Universidad de Chile (FCFM) start-up fund and Chilean CEGA FONDAP CONICYT 15090013 and University of Canterbury's Mason Trust fund for funding, and Fugro NZ for donating the CPT data collection for this research. Jeff Bachhuber, Trevor Hamilton, Chris Hitchcock, Lucy McGee, and Daniel Moncada provided helpful comments to an early version of the manuscript, and thanks to Jarg Pettinga for the support of the research. Thanks to Peter Almond and an anonymous reviewer for their excellent comments and reviews. Finally, data supporting the conclusions of this paper are found in Table 1, Figures 1 and 2, and the supporting information.

References

Almond, P. C., N. T. Moar, and O. B. Lian (2001), Reinterpretation of the glacial chronology of South Westland, New Zealand, *N. Z. J. Geol. Geophys.*, *44*(1), 1–15.

Barnes, P. M., and F. Ghisetti (2013), Offshore faulting and earthquake sources, West Coast, South Island: Stage 2, MBIE Envirolink West Coast Regional Council Advice: 1237-WCRC114, West Coast Regional Council, New Zealand Rep., 34 pp.

Barnes, P. M., H. C. Bostock, H. L. Neil, L. J. Strachan, and M. Gosling (2013), A 2300 paleoearthquake record of the Southern Alpine Fault and Fiordland Subduction Zone, New Zealand, based on stacked turbidites, *Bull. Seismol. Soc. Am.*, *103*, 2424–2446.

Barrell, D. J. A. (2011), Quaternary glaciers of New Zealand, in *Quaternary Glaciations—Extent and Chronology*, edited by J. Ehlers et al., pp. 1047–1064, Elsevier, Amsterdam.

Barth, N. C., D. K. Kulhanek, A. G. Beu, C. V. Murray-Wallace, B. W. Hayward, D. C. Mildenhall, and D. E. Lee (2013), New c. 270 kyr strike-slip and uplift rates for the southern Alpine Fault and implications for the New Zealand plate boundary, *J. Struct. Geol.*, *64*, 39–52, doi:10.1016/j.jsg.2013.08.009.

Beavan, J., P. Denys, M. Denham, B. Hager, T. Herring, and P. Molnar (2010), Distribution of present-day vertical deformation across the Southern Alps, New Zealand, from 10 years of GPS data, *Geophys. Res. Lett.*, *37*, L16305, doi:10.1029/2010GL044165.

Beavan, J. M., et al. (1999), Crustal deformation during 1994–1998, due to oblique continental collision in the central Southern Alps, New Zealand, and implications for seismic potential of the Alpine fault, *J. Geophys. Res.*, *104*(B11), 25,233–25,255, doi:10.1029/1999JB900198.

Berryman, K. R., U. A. Cochran, K. J. Clark, G. P. Biasi, R. M. Langridge, and P. Villamor (2012), Twenty-four surface-rupturing earthquakes over 8000 years on the Alpine fault, New Zealand, *Science*, *36*(6089), 1690–1693, doi:10.1126/science.1218959.

Chandler-Yates, N. (2016), Active Tectonic and Paleoseismic Investigation of the Lower Mikonui Valley in Westland, New Zealand, Unpublished MS thesis, Univ. of Canterbury, Christchurch New Zealand, 133 pp.

Cox, S. C., and D. J. A. Barrell (compilers) (2007), Geology of the Aoraki area: Scale 1:250,000, Lower Hutt: GNS Science, Institute of Geological and Nuclear Sciences 1:250,000 geological map 15, 71 pp. and 1 folded map.

Cox, S. C., M. W. Stirling, F. Herman, M. Gerstenberger, and J. Ristau (2012), Potentially active faults in the rapidly eroding landscape adjacent to the Alpine Fault, central Southern Alps, New Zealand, *Tectonics*, *31*, TC2011, doi:10.1029/2011TC003038.

Davey, F. J. (2010), Crustal seismic reflection profile across the Alpine Fault and coastal plain at Whataroa, South Island, *N. Z. J. Geol. Geophys.*, *53*, 359–368.

Davy, R., T. Stern, and J. Townend (2013), Gravity analysis of glaciotectonic processes, central Alpine Fault, South Island, New Zealand, *N. Z. J. Geol. Geophys.*, *53*(4), 1–9, doi:10.1080/00288306.2013.782324.

De Pascale, G. P., and R. Langridge (2012), New on-fault evidence for a great earthquake in A.D. 1717, central Alpine fault, New Zealand, *Geology*, *40*, 791–794, doi:10.1130/G33363.1.

De Pascale, G. P., T. R. Davies, and M. C. Quigley (2014), Lidar reveals uniform Alpine Fault offsets and bimodal plate boundary rupture behavior, New Zealand, *Geology*, *42*(5), 411–414, doi:10.1130/G35100.1.

DeMets, C., R. G. Gordon, D. F. Argus, and S. Stein (1994), Effect of recent revisions to the geomagnetic reversal time scale on estimates of current plate motions, *Geophys. Res. Lett.*, *21*, 2191–2194, doi:10.1029/94GL02118.

Gage, M. (1945), The Tertiary and Quaternary geology of Ross, Westland, *Trans. R. Soc. N. Z.*, *75*, 138–159.

Ghisetti, F. C., P. M. Barnes, and R. H. Sibson (2014), Deformation of the top basement unconformity west of the Alpine Fault (South Island, New Zealand): Seismotectonic implications, *N. Z. J. Geol. Geophys.*, *57*, 271–294.

Grant, L. B., J. T. Waggoner, T. K. Rockwell, and C. von Stein (1997), Paleoseismicity of the north branch of the Newport-Inglewood fault zone in Huntington Beach, California, from cone penetrometer test data, *Bull. Seismol. Soc. Am.*, *87*(2), 277–293.

Howarth, J. D., S. J. Fitzsimmons, R. J. Norris, and G. E. Jacobsen (2012), Lake sediments record cycles of sediment flux driven by large earthquakes on the Alpine fault, New Zealand, *Geology*, *40*, 1091–1094, doi:10.1130/G33486.1.

Kamp, P. J. J., P. F. Green, and J. M. Tippet (1992), Tectonic architecture of the mountain front-foreland basin transition, South Island, New Zealand, assessed by fission track analysis, *Tectonics*, *11*(1), 98–113, doi:10.1029/91TC02362.

Lund Snee, J. E., V. G. Toy, and B. Gessner (2013), Significance of brittle deformation in the footwall of the Alpine Fault, New Zealand: Smithy Creek Fault zone, *J. Struct. Geol.*, *64*, 79–98.

Marliyani, G. I., T. K. Rockwell, N. W. Onderdonk, and S. F. McGill (2013), Straightening of the northern San Jacinto fault, California, as seen in the fault-structure evolution of the San Jacinto valley stepover, *Bull. Seismol. Soc. Am.*, *103*(3), 2047–2061, doi:10.1785/0120120232.

Nathan, S., H. J. Anderson, R. A. Cook, R. H. Herzer, R. H. Hoskins, J. I. Raine, and D. Smale (1986), *Cretaceous and Cenozoic Sedimentary Basins of the West Coast region, South Island, New Zealand*, *N. Z. Geol. Surv. Basin Stud.*, vol. 1, 90 pp., Department of Scientific and Industrial Research, Wellington, N. Z.

Norris, R. J., and A. F. Cooper (2001), Late Quaternary slip rates and slip partitioning on the Alpine Fault, New Zealand, *J. Struct. Geol.*, *23*, 507–520, doi:10.1016/S0191-8141(00)00122-X.

Robertson, P. K. (1990), Soil classification using the cone penetration test, *Can. Geotech. J.*, *27*(1), 151–158.

Stirling, M. W., et al. (2012), National Seismic Hazard Model for New Zealand: 2010 update, *Bull. Seismol. Soc. Am.*, *102*, 1514–1542.

Suggate, R. P., and P. C. Almond (2005), The Last Glacial Maximum (LGM) in western South Island, New Zealand: Implications for the global LGM and MIS 2, *Quat. Sci. Rev.*, *24*, 1923–1940.

Sutherland, R. (1996), Transpressional development of the Australia-Pacific boundary through southern South Island, New Zealand: Constraints from Miocence-Pliocene sediments, Waiho-1 borehole, South Westland, *N. Z. J. Geol. Geophys.*, *39*, 251–264.

Sutherland, R., et al. (2007), Do great earthquakes occur on the Alpine fault in central South Island, New Zealand?, in *A Continental Plate Boundary: Tectonics at South Island, New Zealand*, *Geophys. Monogr. Ser.*, edited by D. Okaya, T. A. Stern, and F. Davey, pp. 235–251, AGU, Washington, D. C.

Walcott, R. I. (1998), Modes of oblique compression: Late Cenozoic tectonics of the South Island of New Zealand, *Rev. Geophys.*, *36*, 1–26, doi:10.1029/97RG03084.

Wallace, L. M., J. Beavan, R. McCaffrey, K. Berrymany, and P. Denys (2007), Balancing the plate motion budget in the South Island, New Zealand using GPS, geological and seismological data, *Geophys. J. Int.*, *168*, 332–352, doi:10.1111/j.1365-246X.2006.03183.x.

Wells, A., M. D. Yetton, R. P. Duncan, and G. H. Stewart (1999), Prehistoric dates of the most recent Alpine fault earthquakes, New Zealand, *Geology*, *27*, 995–998.

Wells, D. L., and K. J. Coppersmith (1994), New empirical relationships among magnitude, rupture length, rupture width, rupture area, and surface displacement, *Seismol. Soc. Am. Bull.*, *84*, 974–1002.